

Crystal Structure Transformations and Orientation in Crosslinked Elastic Fibers of an Ethylene-Octene Copolymer in Response to Deformation and Heat Treatment

Li-Zhi Liu,¹ Rajesh Paradkar,¹ Selim Bensason²

¹The Dow Chemical Company, 2301 N. Brazosport Blvd., Freeport, Texas 77541

²Dow Europe GmbH, Bachtobelstrasse 3, Horgen, Switzerland

*Present address: Li-Zhi Liu, Beijing Research Institute of Chemical Industry, 14, Beisanhuan Donglu, Chaoyang District, Beijing, China 100013.

Correspondence to: L.-Z. Liu (E-mail: violetlj208@gmail.com)

ABSTRACT: Crosslinked elastic fibers, made from a low density (0.875 g/cc) ethylene-octene copolymer, were studied after constrained at 300% elongation and annealed at different temperatures (40–80°C) to simulate conditions encountered in yarn and textile processing. It is surprisingly found that the transition from pseudo hexagonal to orthorhombic structure is much faster under simultaneously constraining and annealing than that without strain. Almost a neat orthorhombic structure can be produced when the fiber is annealed at 60°C. Annealing above 60°C leads to mixed orthorhombic and pseudo-hexagonal structures. The average melting point increases with an increase in the fraction of orthorhombic phase. It is also surprisingly noted that the simultaneously constraining and annealing of the fiber can produce highly oriented crystals, even annealed at 80°C (above the average melting point of 65°C). The unique effect of annealing under large strain can be attributed to the crosslinking of the fiber, which makes it possible for the fiber to have strong chain orientation (even in molten state) under large strain. The strong chain orientation in melt leads to a faster structural transition from pseudo hexagonal to more stable orthorhombic structure. The strong chain orientation is also very likely the reason why highly oriented crystal and amorphous phases are formed, including the case where the fiber is annealed above melting point. These findings could be leveraged for improving thermal and mechanical properties of the fabrics made with such fibers.

© 2013 Wiley Periodicals, Inc. *J. Appl. Polym. Sci.* 130: 3565–3573, 2013

KEYWORDS: crystallization; X-ray; fibers; polyolefins; textiles

Received 14 December 2012; accepted 8 May 2013; Published online 26 June 2013

DOI: 10.1002/app.39533

INTRODUCTION

It has been reported that an ethylene-octene copolymer, with a density of 0.875 g/cc, typically cannot crystallize into lamellae due to the high level of short chain branching.^{1,2} A fringe micelle or bundle-like crystal morphology has been proposed.² It is known that the presence of octene comonomer leads to considerable distortion of the polyethylene crystal lattice. Compared with a polyethylene homo-polymer, there is a significant decrease in X-ray diffraction intensity of the (110) reflection, whereas the (200) reflection merely appears as a shoulder in the wide angle X-ray diffraction pattern.³ In addition to the (110) and (200) orthorhombic reflections, another peak with a *d*-spacing between 4.46 and 4.52 Å can be also observed in some cases. This reflection is generally attributed to the presence of pseudo hexagonal crystallites.⁴ Previous studies have shown that a substantial degree of methyl, and a small portion of ethyl branches can be accommodated in the orthorhombic lattice, but hexyl side chains

cannot be incorporated in the orthorhombic crystal lattice to any degree.^{3–6} In linear polyethylene, the hexagonal structure is a mesophase and likely occurs in ethylene-octene copolymers, in order to accommodate some of the hexyl side chains.³ It is also worth mentioning that, although the hexagonal mesophase is metastable, in linear polyethylene, at room temperature, it has been found to be stable in ethylene-propylene copolymers, i.e., the presence of the side chain defects appears to stabilize the hexagonal form at lower temperatures. A study by de Ballesteros et al.⁷ on ethylene-rich ethylene-propylene copolymers demonstrated that the insertion of the propylene moiety in the lattice of orthorhombic crystal structure from the ethylene sequence gradually increased the disorder in the crystalline phase and eventually led to a pseudo-hexagonal crystalline structure at high propylene content. In other words, depending on the composition of the copolymer, the crystalline structure could be different and even have mixed orthorhombic and pseudo hexagonal structures.^{8–10}

© 2013 Wiley Periodicals, Inc.

Low crystallinity ethylene alpha-olefin copolymers can be made into crosslinked elastic fibers, with unique performance attributes, for textile applications, which are described in detail by Casey et al.¹ Crosslinking leads to a network of covalently bonded polymer chains and imparts mechanical integrity to the fiber at elevated temperatures. In this work, crosslinked elastic fibers, made of ethylene-octene copolymer with density and melt index of 0.875 g/cc and 3.0 deg/min (190°C, 2.16 kg), respectively, were studied with Wide Angle X-ray Diffraction (WAXD), Differential Scanning Calorimetry (DSC) and birefringence. The fibers were studied after annealed at different temperatures and constrained at 300% elongation to simulate conditions encountered in yarn and textile processing. The present study shows that simultaneously constraining (300% elongation) and annealing (40 to 80°C) the cross-linked fiber can make the structural transition from pseudo hexagonal to orthorhombic structure much faster than without strain. It is also surprisingly noticed that maintaining the strain of 300% and annealing the fiber (even above the average melting point) can produce highly oriented crystal and amorphous phases. This study provides insights into the micro structural basis for the fiber response during fabric processing (a simultaneous heating and stretching). The mechanism is proposed for the unusual structural change in response to simultaneous heating and stretching. The findings could be leveraged for improving the thermal and mechanical properties of the fabrics made with the fiber.

EXPERIMENTAL

Materials and Sample Preparation

An ethylene-octene copolymer (13% mol octene) with density of 0.875 g/cc and 3°/min melt index (190°C, 2.16 kg) was used for making the fiber studied in this work. The copolymer was made with INSITE constrained geometry catalyst technology. The fibers were melt spun into 70 denier (about 0.1 mm in diameter) monofilaments and subsequently crosslinked via e-beam irradiation (19.2 MRad dose). The crosslinked gel fraction, as measured by boiling xylene extraction per ASTM D2765, was 70%. For X-ray diffraction measurements, 10 fibers were aligned into a bundle, ~10 cm in length. The fiber bundle was stretched to four times its original length (300% elongation) and then mounted on a cardboard frame. Some of the samples were annealed at various temperatures (40–100°C) by placing the framed bundles into a temperature equilibrated convection oven for 15 min, followed by cooling to ambient temperature. It should be noted that annealing at temperatures 60, 80, and 100°C was essentially carried out in partially melted and/or oriented state.

Wide Angle X-ray Diffraction (WAXD)

The fibers were analyzed using D8 Discover diffractometer from Bruker-AXS, equipped with General Area Detector Diffraction System (GADDS) and a video microscope with a laser pointer. The core of GADDS is the high-performance HI-STAR two-dimensional (2D) detector. Detector resolution was 1024x1024-pixel. The sample-to-detector distance was 6 cm. Data were collected using copper (K α) radiation through a 0.3 mm pinhole collimator. A well-aligned region of the fiber bundle was identified with the help of a video microscope. This region with parallel fibers was chosen for X-ray measurements. The collected WAXD images were calibrated using corundum standard.

Differential Scanning Calorimetry (DSC)

To determine effect of stretching and annealing on the melting characteristics, DSC measurements were performed in a stretched state, by winding deformed fibers onto miniature brass pulleys and tying the ends to maintain the deformation throughout the scan, as described by Lyon et al.¹¹ Fibers were stretched by means of a static weight to produce the desired elongation and then wound onto brass pulley of ca. 500 mg weight machined to fit into standard aluminum DSC pans. DSC Measurements were performed with a TA Instruments Q1000 DSC. The instrument was calibrated using indium (melting point = 156.6°C, heat of fusion = 28.4 J/g) following standard procedures. The samples were first cooled down to -40°C and were then heated to 150°C at a rate of 10°C/min.

Birefringence Measurement

Fiber birefringence was measured using a Nikon polarized light microscope equipped with a Berek tilting compensator. The detailed procedure for estimating the birefringence using a Berek compensator is described in Berek Compensator Instructions [Nikon Corporation, Japan (2001)]. Briefly, the fiber was mounted on a glass slide. A drop of UV curable optical adhesive (Norland, 61) was placed on the fiber. The fiber was covered with a glass cover slip and the adhesive cured in long wavelength UV light for 3 min. The sample was then oriented between cross polarizers such that the fiber axis was 45°, with respect to the axis of both, the polarizer and the analyzer. The compensator was adjusted, by turning the drum, until a black fringe appeared at the point of interest in the fiber. The black fringe becomes visible when the retardation of the compensator is equal and opposite the retardation, at the point of interest, in the fiber. A table supplied with the Berek compensator was used to obtain the retardation corresponding to the drum position. Fiber diameter was measured at five different points along the length of the fiber using Image Pro Express software and the average was used to calculate the fiber birefringence using the equation shown below:

$$R = (N_{||} - N_{\perp}) * t \quad (1)$$

where R is the optical path length difference or retardation, $N_{||}$ and N_{\perp} are the refractive indices parallel and perpendicular to the fiber axis, and t = thickness of the fiber. Therefore R/t is the birefringence ($N_{||} - N_{\perp}$).

RESULTS AND DISCUSSION

Structure of Crosslinked Fiber Without Annealing and Stretching

The two dimensional WAXD pattern of the original control fiber, not subjected to annealing and stretching, is shown in Figure 1. It is seen from the figure that strong diffraction is seen near the equatorial diffraction, indicating that the crystals are oriented. The corresponding profiles in the fiber and equatorial directions are also shown in the figure. The diffraction profile obtained from equatorial direction has two diffraction peaks. The small peak at $2\text{-theta} = 23^\circ$ (with Cu radiation) is from orthorhombic (200) structure. The main diffraction peak at $2\text{-theta} \sim 19.5^\circ$ is primarily from the pseudo hexagonal (100) peak. The pseudo hexagonal (100) peak also partially overlaps with the orthorhombic (110) peak, which typically appears

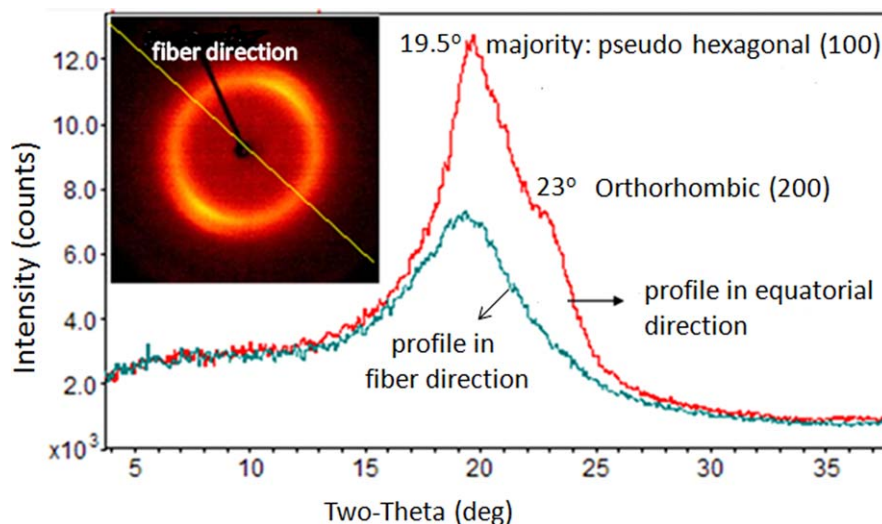


Figure 1. Diffraction pattern and profiles in fiber and equatorial directions of the original fiber (cross-linked, but not subjected to annealing and stretching). [Color figure can be viewed in the online issue, which is available at wileyonlinelibrary.com.]

around $2\text{-theta} = 21.3^\circ$. This could explain why the (110) main peak from orthorhombic structure of PE is not visible. The results from the original fiber (crosslinked, but not subjected to annealing and stretching) indicate that both pseudo hexagonal and orthorhombic crystal structures exist in the fiber, and that the majority of the crystals have hexagonal structure based on the observed difference in diffraction intensity. Compared with earlier study⁹ on similar copolymer without crosslinking, this study shows that crosslinking does not have that much effect on crystalline structure of the copolymer.

EFFECT OF STRETCHING AND ANNEALING ON CRYSTAL STRUCTURE AND ORIENTATION

Effect of Stretching

The cross-linked fiber was first studied by stretching to 300% strain at room temperature. Upon stretching, the broad diffraction arc in Figure 1 for unstretched control fiber is replaced by

a small spot in equatorial direction (Figure 2), indicating that the crystals are much more oriented after stretching to 300% strain. By changing the image contrast, two weak diffraction maxima near 36° are also observed (lower image in Figure 2). As the (110) peak of the hexagonal structure and the (020) peak of orthorhombic structure are near 36° for copper radiation,¹ the weak diffraction spots in equatorial direction (near detector edge) could have contribution from both structures. However, it is more likely they are associated mainly with the hexagonal structure, as the main diffraction peak is at $2\text{-theta} = 20.2^\circ$ (Figure 2). Comparing the diffraction peak at 23° , before and after stretching (Figures 1 and 2), it is seen that the peak at 23° before deformation is almost lost after deformation, indicating a decrease in orthorhombic structures due to the stretching. A similar crystal structure transition from orthorhombic to hexagonal, under deformation, was also previously observed for an ethylene-propylene random copolymer (78 wt%

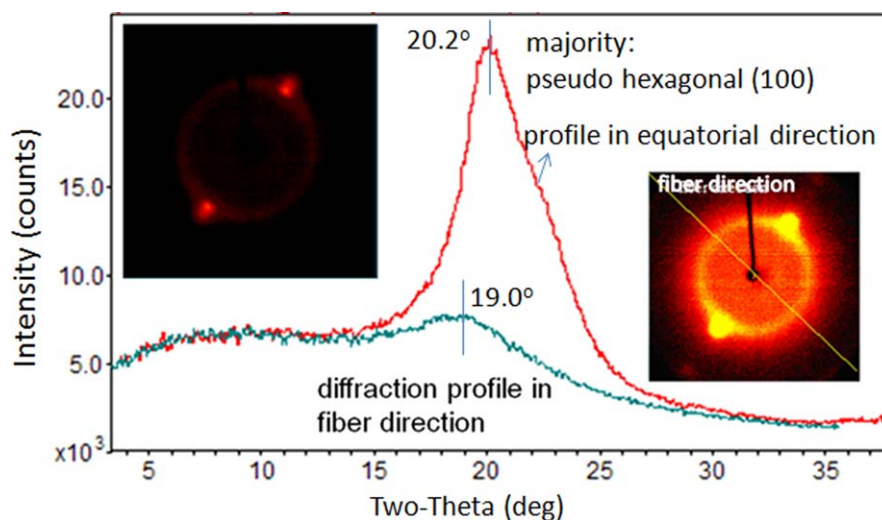


Figure 2. Diffraction pattern and profiles of the cross-linked fiber constrained at 300% stain at room temperature. [Color figure can be viewed in the online issue, which is available at wileyonlinelibrary.com.]

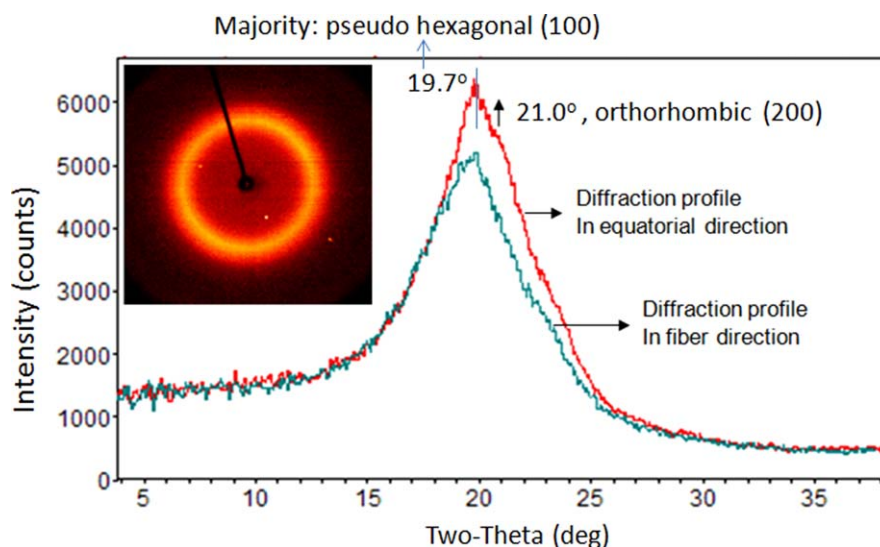


Figure 3. Diffraction pattern and profiles of the cross-linked fiber constrained at its original length and exposed to 80°C in air for 15 min. [Color figure can be viewed in the online issue, which is available at wileyonlinelibrary.com.]

or 85 mol% of ethylene moiety).⁹ In this study, Liu et al. found, that even with very small strain, such as 0.12%, the deformation could completely transform the orthorhombic crystals into the pseudo hexagonal form. Since the required strain was very low, the authors believe that the transformation from orthorhombic to hexagonal structures is most likely a solid-to-solid phase transition, instead of going through the amorphous state and then re-crystallizing into the hexagonal structure. By comparing the images from Figures 1 and 2, it is also seen that after stretching, the crystals are significantly more oriented.

Effect of Annealing

The cross-linked fiber was also annealed at 80°C in air for 15 min, while constrained at its original length (no shrinkage was allowed). The diffraction pattern and profiles are shown in Figure 3. The diffraction image indicates that the crystal orientation was almost completely lost after annealing. In fact, very little intensity difference is observed in the scattering profiles, obtained in equatorial and fiber directions, suggesting that only slight overall orientation exists after annealing at 80°C. Comparing Figure 1 (control sample without annealing) and Figure 3, it is noted that after annealing at 80°C for 15 min, a weak diffraction peak from orthorhombic structure at 21° is observed. This suggests that annealing at 80°C, (above the average melting point of the fiber and no shrinkage was allowed) can promote formation of the orthorhombic crystal structure. The mechanism is discussed in details in next section.

EFFECT OF SIMULTANEOUS STRETCHING AND ANNEALING ON CRYSTAL STRUCTURE AND ORIENTATION

Transition in Crystalline Structure

Figure 4 shows the two dimensional diffraction patterns and diffraction profiles, obtained in equatorial direction for the control fiber (no strain, no annealing) and the fiber constrained at 300% elongation and annealed at 40°C for 15 min. It can be seen from the figure that the crystal orientation after

stretching and annealing is much higher than in the control fiber. By comparing the diffraction profiles in Figure 4, it can be seen that annealing at 40°C increased the orthorhombic phase. This increase is represented by the presence of a strong (110) diffraction peak at 2-theta around 21°. In contrast to that, the fraction of hexagonal phase decreased as evidenced by a decrease in the diffraction intensity at 2-theta = ~19.7°. The diffraction profiles in fiber and equatorial direction are shown in Figure 5 for the fiber annealed at 60°C. It can be seen that the diffraction is oriented in equatorial direction. The profile fitting in equatorial direction shows two well-defined peaks with main diffraction peak at 2-theta = 21° and 2nd one at 2-theta = 23° (Figure 5). As copper radiation was used, these two diffraction peaks suggest a nearly pure orthorhombic crystal structure. This is quite surprising that after annealing at 60°C for only 15 min at 300% strain, the crystal structure changed from mainly hexagonal to almost a neat orthorhombic. A comparison of the orthorhombic structure formed by annealing the fiber at 40 and 60°C, is shown in Figure 6. The (110) diffraction peak from orthorhombic structure after annealing at 60°C is shifted to a larger angle, indicating closer crystal packing (smaller *d*-spacing) for the corresponding crystal planes. The much sharper (110) diffraction peak observed after annealing at 60°C indicates that the crystal size across the fiber section, is significantly larger than after annealing at 40°C.

Figure 7 shows the diffraction profiles in fiber and equatorial direction of the fiber annealed at 80°C. It is seen from the scattering image that the crystals are still very oriented. The profile fitting result for the diffraction profile in equatorial direction is also shown in Figure 7. The diffraction peaks, 2-theta = 21.0° and 2-theta = 23.0°, correspond to (110) and (200) peak of orthorhombic structure, respectively. The peak at 2-theta = 19.5° is the contribution from (100) diffraction of pseudo hexagonal structure. That is, annealing at 80°C with 300% strain results in mixed orthorhombic and hexagonal

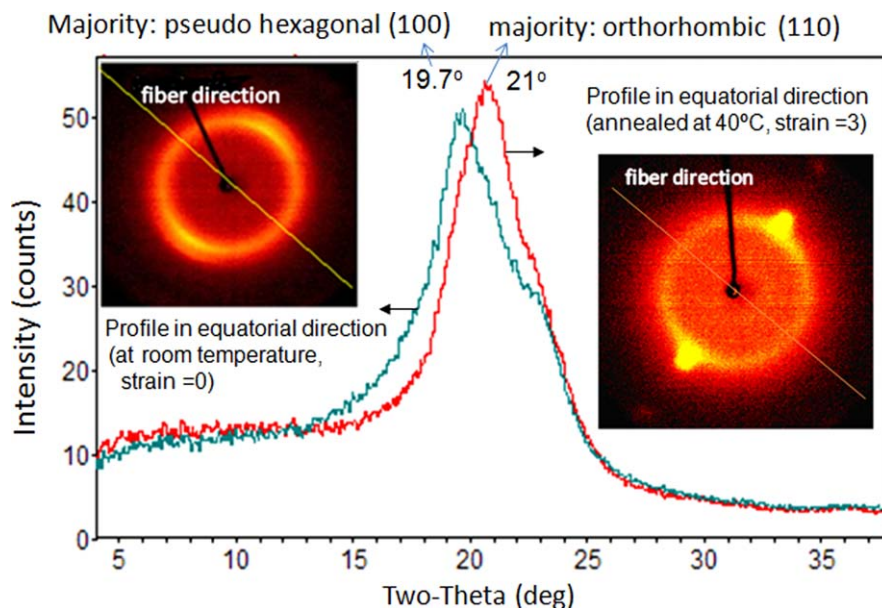


Figure 4. Diffraction patterns and profiles of cross-linked fiber constrained at strain of 300% and annealed at 40°C for 15 min, compared with that of control fiber not subjected to annealing and stretching. [Color figure can be viewed in the online issue, which is available at wileyonlinelibrary.com.]

structures again. However, in contrast to the mixed structure produced after annealing at 40°C (Figure 5), more crystals with orthorhombic structure was obtained when annealing at 80°C. Moreover, the orthorhombic crystals, obtained when annealing at 80°C, were better defined with significantly larger size (sharper peaks).

In summary, constraining (300% strain) and annealing (40 to 80°C range) the fibers for 15 min can cause a structural transition from pseudo hexagonal to orthorhombic. This transition is initiated at 40°C and results in a nearly neat orthorhombic structure after annealing at 60°C. A further increase in the annealing temperature to 80°C results in a lower fraction of orthorhombic structure, but it is still a dominant phase. In a published study on a similar material (ethylene-propylene random copolymer

with 78 wt% of ethylene moiety), Liu et al.,⁹ showed that the copolymer, isothermally crystallized at 20°C, forms a pseudo hexagonal structure. An orthorhombic structure is formed when the same copolymer is isothermally crystallized at 50°C (under no strain), although it takes much longer to get the neat orthorhombic structure. The study also suggests that crystallization at room temperature favors the formation of smaller crystals with the metastable pseudo hexagonal structure, and the slower crystallization process at high temperature favors formation of the orthorhombic structure. This work shows that a transition from the pseudo hexagonal to orthorhombic structure is also observed when annealing at 80°C (under no strain, Figure 3). However, this transition is much less intense compared to the transition observed when the fiber is under a strain of 300% and annealed

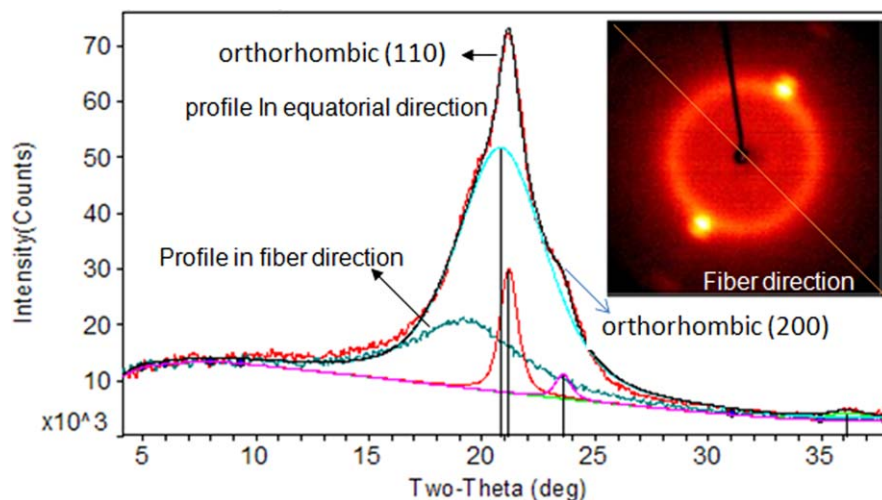


Figure 5. Diffraction pattern and profiles of the cross-linked fiber constrained at 300% strain and exposed at 60°C in air for 15 min. [Color figure can be viewed in the online issue, which is available at wileyonlinelibrary.com.]

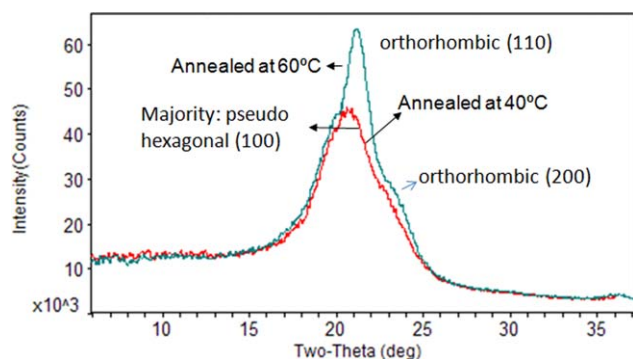


Figure 6. Diffraction profiles in equatorial direction of the fiber stretched to 300% elongation and annealed at 40 and 60°C, respectively. [Color figure can be viewed in the online issue, which is available at wileyonlinelibrary.com.]

at 80°C. This indicates that orientation plays a major role in the crystal transition from pseudo hexagonal to orthorhombic structure at high temperature. In other words, existing orientation can promote the structural transition from a pseudo hexagonal to orthorhombic structure much faster.

Crystal and Amorphous Orientation

The chain orientation in the crystalline (f_c) and amorphous phases (f_a) can be calculated using the Hermans' orientation function¹²

$$f_c = \frac{3\langle \cos^2 \phi \rangle - 1}{2} \quad (2)$$

where ϕ is the angle between the chain axis and a reference axis and $\langle \cos^2 \phi \rangle$ is defined as:

$$\langle \cos^2 \phi \rangle = \frac{\int_0^{\pi/2} I(\phi) \cos^2 \phi \sin \phi \, d\phi}{\int_0^{\pi/2} I(\phi) \sin \phi \, d\phi} \quad (3)$$

$I(\phi)$ is the scattered intensity along the angle ϕ . In the present work, fiber direction was used as the reference direction and f_c

represents the degree of crystal orientation along fiber direction. A value of 1 represents perfect orientation, 0 represent random orientation, and -0.5 represents perfectly perpendicular orientation.

It should be pointed out that the average melting point of the cross-linked fiber was about 65°C (see next section for thermal study). Therefore, one would expect a significant decrease in the degree of crystal orientation, after annealing at 60 and 80°C, due to the partial melting of the fiber. This effect should be especially pronounced for the sample annealed at 80°C. However, the diffraction patterns in Figures 5 and 7 indicate that crystals are still very high oriented. For the (110) diffraction peak near 2-theta = 21°, the calculated Herman function values are -0.42 and -0.39 for the fiber annealed at 60 and 80°C, respectively. As the normal on the (110) lattice plane of a polyethylene crystal is perpendicular to the chain direction, the following equation is valid¹²

$$f_{110} = -0.5f_c \quad (4)$$

That is, the f_c is 0.84 and 0.78, respectively. This quantitatively confirms that constrained annealing under strain close to or above the average melting point (65°C) of the cross-linked fiber, not only leads to a nearly complete conversion of the crystal from pseudo hexagonal to orthorhombic, but the crystals remain very oriented. The evaluation also indicated that the crystals were more oriented when the fiber was annealed at 60 than 80°C.

The orientation of amorphous segments can also be evaluated from the X-ray data with Herman's orientation function.¹² However, in case of mixed orthorhombic and pseudo hexagonal crystal phases in the fiber (such as, for the sample annealed at 80°C), the peak maxima of amorphous polyethylene segments (around 19.5° for copper radiation) overlaps a lot with the (100) peak around 20° for the pseudo hexagonal structure. In this case, it is difficult to evaluate the amorphous orientation using Herman's orientation function. In

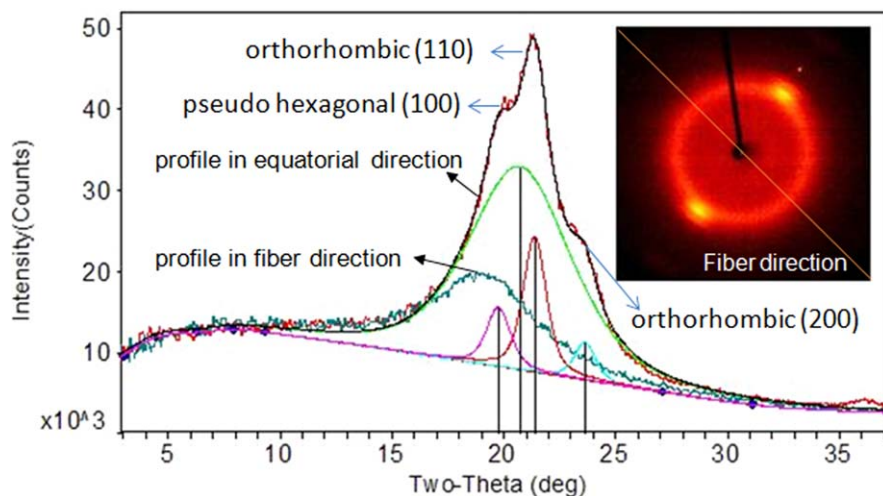


Figure 7. Diffraction pattern and profiles of the cross-linked fiber constrained at 300% stain and exposed at 80°C in air for 15 min. [Color figure can be viewed in the online issue, which is available at wileyonlinelibrary.com.]

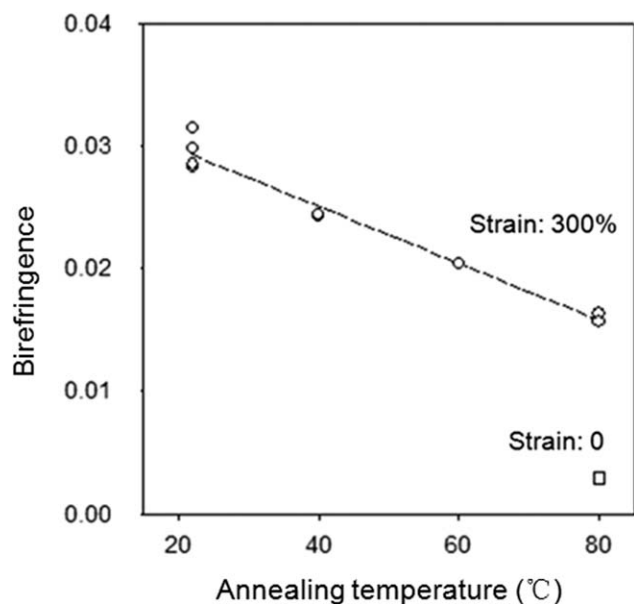


Figure 8. Birefringence of the control fiber (no strain) annealed at 80°C and the fiber constrained at 300% strain and annealed at different temperatures.

the present work, a different approach was used to compare the amorphous orientation for the fiber annealed at 60 and 80°C. As the amorphous scattering power in the equatorial direction is related to the amorphous segments aligned in the fiber direction and the amorphous scattering power in the fiber direction is related to the amorphous segments aligned in the equatorial direction, the ratio of the scattering power in these two directions is related to the amorphous orientation. The better the alignment of amorphous segments in the fiber direction is, the higher the amorphous scattering in equatorial direction. In the present work, the amorphous scattering power (the area of the amorphous halo) in the fiber direction (average of 10°) and equatorial direction (average of 10°) obtained by profile fitting were used to evaluate the relative amorphous orientation. An amorphous orientation index, f_a , was defined as the ratio of amorphous scattering area in the fiber direction, A_{fiber} , to the scattering area in the equatorial direction, $A_{\text{equatorial}}$, as shown in the equation below:

$$f_a = 1 - (A_{\text{fiber}}/A_{\text{equatorial}}) \quad (5)$$

A value of 1 represents perfect amorphous orientation and a value of 0 represents completely random orientation. The fitted diffraction profiles in the equatorial direction for the fiber annealed at 60 and 80°C are shown in Figures 6 and 7, respectively. The calculated amorphous orientation index is 0.77 for the fiber annealed at 60°C and 0.51 when annealed at 80°C. That is, like the crystals, the amorphous segments are also less oriented in the fibers annealed at 80°C as compared with those annealed at 60°C. In summary, when annealed at 60°C and a nearly neat orthorhombic structure was obtained; both crystal and amorphous segments were more oriented than the fiber annealed at 80°C.

The orientation of amorphous segments and the average distance of neighboring amorphous segments are related. For isotropic polyethylene material, the average amorphous inter-chain distance is about 4.5 Å, and the peak maximum is near 19.5° with copper radiation. For an oriented fiber, the average inter-chain distance of the amorphous segments is different in different directions. As shown in Figures 5 and 7, the peak position of amorphous scattering in the fiber and equatorial directions can be significantly different. For the fibers annealed at 60 and 80°C under 300% strain, the average d-spacing of neighboring amorphous segments in the equatorial direction is 4.6 Å based on the peak at 19.2° in the profile obtained in fiber direction. However, the average distance of neighboring amorphous segments aligned in the fiber direction is only around 4.3 Å, based on the peak at 20.8° in the profile obtained in equatorial direction.

Overall Fiber Orientation

Because of mixed crystal phases or ill defined crystalline structures, it is difficult to evaluate the crystal and amorphous orientation for all the fiber samples. A birefringence study was also carried out to measure the overall fiber orientation after annealing at different temperatures with strain of 3. As shown in Figure 8, the birefringence decreases with an increase in annealing temperature, indicating a decrease in the overall orientation. However, the overall orientation is still very high even after annealing at 80°C, where about 95% of original crystals are melted (see the thermal study in next section). In fact, the birefringence at 80°C for un-stretched sample (maintaining zero strain) is very low (Figure 8) and suggests a near total loss of the entire orientation, which was consistent with WAXD results shown in Figure 3. By comparing X-ray data for the fibers annealed at 60 and 80°C with the birefringence data, the same trend was observed, i.e., the overall orientation decreased with an increase in the annealing temperature, but even annealing at 80°C while maintaining the strain of 300% can indeed produce highly oriented crystals.

In summary, the faster structural transition and highly oriented crystal and amorphous phases obtained at near and above its average melting point can be attributed to the crosslinking of the fiber. It is supposed to be the networking that makes it possible to lead to strong chain orientation under large strain, especially in molten state (above average melting point of the fiber). The strong chain orientation in melt is very likely to lead to faster structural transition from pseudo hexagonal to better defined orthorhombic structure. The strong chain orientation could be the reason why highly oriented crystal and amorphous phases are observed for the fiber annealed above melting point.

MELTING BEHAVIOR

The melting behavior of the fiber simultaneously stretched and annealed can provide additional information on two different crystals and distribution, as well as crystal size. To study the effect of stretching on the melting characteristics, DSC measurements were performed in a stretched state, by winding deformed fibers onto miniature brass pulleys and tying the ends

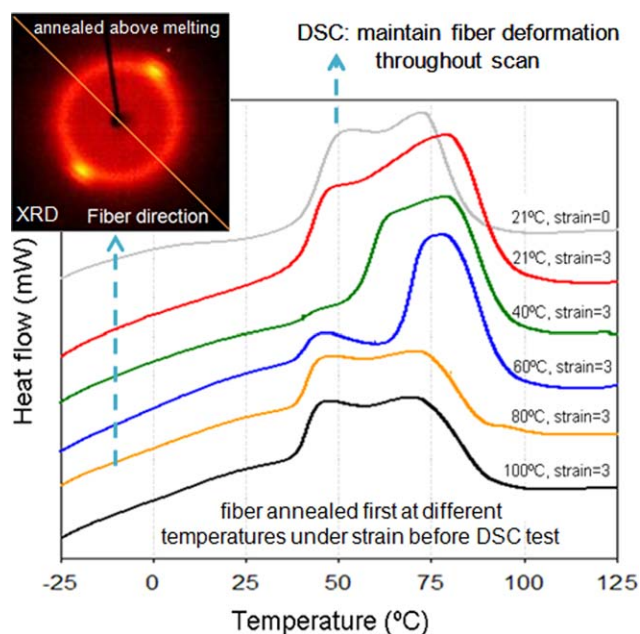


Figure 9. DSC thermograms of the cross-linked fiber annealed at different temperatures. [Color figure can be viewed in the online issue, which is available at wileyonlinelibrary.com.]

to maintain the deformation throughout the scan, as described by Lyon et al.¹¹ Maintaining deformation during a thermal scan allowed better comparison of the X-ray diffraction and thermal data, since they were obtained under the same strain conditions. DSC thermograms of samples annealed at different temperatures are shown in Figure 9. The crystallinity obtained from the thermogram of original fiber without annealing and stretching was about 15%. The fiber not subjected to annealing and stretching shows a broad DSC melting peak, ranging from 40 to ca. 90°C. The broad peak from the control fiber (crosslinked, no annealing and stretching) actually consists of two melting peaks with peak positions at 53 and 73°C, respectively. The structure study in the previous section could be very helpful in terms of understanding the complicated melting behavior. The X-ray study shows that when the fiber is annealed at high temperature, much faster (less than 15 min) structural transition from pseudo hexagonal to orthorhombic can occur, due to strong orientation induced by large strain (300%). This suggests that during a DSC heating process, structural transition could happen considering that it takes several minutes to heat the sample from 30 to 80°C at 10°C/min. It is believed that the appearance of the two peaks observed from DSC could be representative of melting of one phase and transforming into a more stable phase followed by melting of the stable phase. For the fiber, which was stretched to 300% elongation but did not annealed at high temperature, the average melting point increased appreciably, as shown in Figure 9. The higher melting point increased from 73 to 80°C, compared with the control fiber (no stretching and no annealing). This could be caused by the effect of strain-induced crystallization where larger hexagonal crystals were formed due to strong orientation. X-ray study shows annealing the fiber at 40°C significantly increased the orthorhombic crystal, as shown in Figure 4. The corresponding

DSC scan shows a significantly narrower melting peak than the two samples without annealing. The annealing at 40°C also lead to an appreciable higher average melting point (73°C, no separated two peaks seen) than the fibers without annealing, as shown in Figure 9. The increase in the average melting point presumably due to the significant conversion of pseudo hexagonal crystal to orthorhombic crystal.

A much narrower melting peak was observed for the fiber annealed at 60°C and can also be explained together with learning from X-ray study. As almost a neat and stable orthorhombic crystal structure was obtained for the fiber annealed at 60°C, no significant structural transition from one phase to a more stable phase would occur during DSC heating process. As the result, a much narrower main melting peak around 78°C, representing mainly the melting of the stable orthorhombic structure, was observed. The appreciably higher average melting point of 78°C was due to a nearly neat orthorhombic structure formed when annealed at 60°C. It should be noted that the DSC melting show a small peak at significant lower temperature (45°C) for the fiber annealed at 60°C. This suggests the presence of a very small fraction of pseudo hexagonal crystals in the sample. The small fraction of pseudo hexagonal crystals could contribute to the left hand asymmetry of the main diffraction peak in Figure 5, as well as a slight shoulder at $2\text{-}\theta=19.5\text{--}19.7^\circ$.

Annealing at 80°C would melt most of the crystals based on the melting profile for the fiber constrained at 300% strain. Most crystals might not be formed during annealing, but during subsequent cooling, as the majority of the crystals melt before 80°C. Annealing at 100°C might actually melt all the crystallites and lead to a total recrystallization during cooling with large strain (300%). The X-ray study shows that the fiber annealed at 80°C has mixed pseudo hexagonal and orthorhombic structures. Therefore, for a heating process, the melting of unstable pseudo hexagonal phase and the transformation into a stable orthorhombic phase could be expected based on the above discussions. This structural transition presumably led to broad melting with two peaks (Figure 9). X-ray study show less orthorhombic crystals were observed for fiber annealed in 80°C than in 60°C. The DSC data is consistent with the finding by X-ray. The same mechanism could apply to shallower melting peaks for the fibers annealed at 100°C.

In summary, the crystal structures in the fiber determine the melting behavior. The neat and stable orthorhombic structure is associated with a very narrow melting peak and a higher average melting point. While less stable pseudo hexagonal structure is associated with a significantly lower melting point, which could be also a narrow peak, such as the small peak with a lower melting point for the fiber annealed at 60°C. Mixed two structures are associated with broad melting, typically represented by two overlapped peaks. The X-ray and DSC data support the conclusion that the appearance of the two peaks observed from DSC is due to melting of one phase and transforming into a more stable phase followed by melting of the stable phase. The shape of the broad melting is supposed to be related to the two crystal fractions.

CONCLUSIONS

1. Simultaneously constraining (300% strain) and annealing (40 to 80°C range) the cross-linked fiber, made from a low density (0.875 g/cc) ethylene-octene copolymer, can make the structural transition much faster (in a range of 15 min vs. days compared with no strain⁹).
2. Annealing and constraining the crosslinked fiber can produce highly oriented crystal and amorphous phases with a higher average melting point, even if the annealing temperature is above the average melting point of the crosslinked fiber. The overall orientation shows a linear decrease as increase in annealing temperature, as evidence by birefringence measurements.
3. A nearly neat orthorhombic structure with highly oriented crystal and amorphous phases was obtained after annealing the fiber at 60°C with 300% strain for only 15 min. Further increase in the annealing temperature to 80°C leads to mixed hexagonal and orthorhombic structures with orthorhombic structure being dominant form.
4. The thermal study shows that annealing the fiber at 40–60°C with 300% strain leads to significantly higher average melting point, especially for the fiber annealed at 60°C where the average melting point (about 75°C) is about 10°C higher than the original fiber.
5. The faster structural transition and highly oriented crystal and amorphous phases obtained at near and above its average melting point can be attributed to the crosslinking of the fiber, which makes it possible to gain strong chain orientation under large strain in molten state (above average melting point of the fiber). The strong chain orientation in melt can lead to faster structural transition from pseudo hexagonal to better defined orthorhombic structure. The strong chain orientation is very likely the reason why highly

oriented crystal and amorphous phases are observed for the fiber annealed above melting point. The findings above could be used for improving the thermal and mechanical properties of the fabrics made with such fibers.

REFERENCES

1. Casey, P.; Chen, H.; Poon, B.; Bensason, S.; Menning, B.; Liu, L.; Hu, Y.; Hoenig, W.; Gelfer, M.; Dems, B.; Rego, M. *Polym. Rev.* **2008**, *48*, 302.
2. Bensason, S.; Minick, J.; Moet, A.; Chum, S.; Hiltner, A.; Baer, E. *J. Polym. Sci. Part B: Polym. Phys.* **1996**, *34*, 1301.
3. Androsch, R.; Blackwell, J.; Chvalun, S. N.; Wunderlich, B. *Macromolecules* **1999**, *32*, 3735.
4. Mathot, V. B. F.; Scherrenberg, R. L.; Pijpers M. F. J.; Bras, W. *J. Thermal Anal.* **1996**, *46*, 681.
5. McFaddin, D. C.; Russell, K. E.; Wu, G.; Heyding, R. D. *J. Polym. Sci. Part B: Polym. Phys.* **1993**, *31*, 175.
6. Wagner, J.; Phillips, P. J. *Polymer* **2001**, *42*, 8999.
7. de Ballesteros, O. R.; Auriemma, F.; Guerra, G.; Corradini, P. *Macromolecules* **1996**, *29*, 7141.
8. Shan, H.; White, J. L. *J. Appl. Polym. Sci.* **2004**, *93*, 9.
9. Liu, L.; Hsiao, B.; Ran, S.; Fu, B. X.; Toki, S.; Zuo, F.; Tsou, A. H.; Chu, B. *Polymer* **2006**, *47*, 2884.
10. Zuo, F.; Burger, C.; Chen, X.; Mao, Y.; Hsiao, B.; Chen, H.; Marchand, G.; Lai, S.-Y.; Chiu, D. *Macromolecules* **2010**, *43*, 1922.
11. Lyon, R. E.; Farris, R. J.; MacKnight, W. J. *J. Polym. Sci. Polym. Lett. Ed.* **1983**, *21*, 323.
12. Hong, K.; Strobl, G. *Macromolecules* **2006**, *39*, 268.